

## Elastic constants of bcc $^4\text{He}$

D. S. Greywall

*Bell Laboratories, Murray Hill, New Jersey 07974*

(Received August 28 1975)

Longitudinal and transverse sound velocities were measured in single crystals of bcc  $^4\text{He}$  with known orientation at  $21.00\text{ cm}^3/\text{mole}$  and at  $1.612\text{ K}$ . In addition, the temperature dependence of the sound velocities along an isochore and along the melting curve was measured for several samples. No premelting effects were observed. These data were used to determine mode Grüneisen parameters. A least-squares fitting of the data at  $1.612\text{ K}$  yielded the reduced adiabatic elastic constants, in units of  $10^5\text{ m}^2/\text{sec}^2$ ,  $C_{11}/\rho = 1.630 \pm 0.036$ ,  $C_{12}/\rho = 1.473 \pm 0.034$ , and  $C_{44}/\rho = 1.137 \pm 0.010$ . These moduli imply a compressibility of  $(3.437 \pm 0.072) \times 10^{-3}\text{ bar}^{-1}$  and a Debye temperature of  $19.17 \pm 0.05\text{ K}$ . The ratios of the corresponding bcc  $^3\text{He}$  to  $^4\text{He}$  elastic moduli at the same molar volume are considerably larger than the classical ratio of unity but in excellent agreement with the quantum-mechanical calculations of Horner. Existing calorimetric data are compared with the present determination of the Debye temperature.

### I. INTRODUCTION

Solid helium is labeled a *quantum solid*<sup>1</sup> owing to the very large quantum-mechanical zero-point motion of the atoms in low-density samples. Because the mean displacements are a significant fraction of the atomic spacing, it might be expected that these solids would possess some very strange and perhaps unique properties. Yet what is observed is that in most respects solid helium behaves macroscopically quite like an ordinary solid.<sup>2</sup> Its crystal structures, thermodynamic properties, and phonon spectra are not particularly unusual. In the hcp phases of  $^3\text{He}$  and  $^4\text{He}$  it is even found that the isotopic ratio of the Debye temperatures is close to the classical value.<sup>3,4</sup> But, although the measured properties of solid helium are in general not unusual, the theoretical understanding of these physical properties is far from complete. The first-principles calculations for solid helium are complicated since the theory must treat both anharmonic forces and short-range correlations of the atomic motions.<sup>5</sup>

The most complete test of any of the various calculations is a comparison of the predicted with the measured phonon dispersion relations. In the case of  $^3\text{He}$ , however, neutron scattering measurements are very difficult because of the large-neutron-absorption cross section of  $^3\text{He}$ . For this isotope, and only in the bcc phase, experimental information about the dispersion curves is at present limited to the slopes of the spectra near the zone center corresponding to the measured ultrasonic sound velocities<sup>6,7</sup> in crystals of known orientation. In the case of  $^4\text{He}$ , neutron-scattering<sup>8-10</sup> and sound-velocity measurements<sup>6,11</sup> provide complementary information. In this paper we will be concerned only with sound-velocity measurements which by themselves still provide a very strict test for any theory of solid helium.

A proper theory must be able to predict correctly not only the sound velocities at a single density but the density and isotopic dependences of these velocities as well.

Sound-velocity measurements are also important since they can be used to provide the only accurate determination of the Debye temperatures  $\Theta_0$  at  $0\text{ K}$  in bcc  $^3\text{He}$  and  $^4\text{He}$ . In  $^3\text{He}$  there are both high- and low-temperature anomalies<sup>3,12,13</sup> in the specific heat which make the determination of  $\Theta_0$  from these data highly uncertain. In  $^4\text{He}$ , the calorimetric measurements<sup>14-18</sup> can only be used to make rough estimates of  $\Theta_0$  since the bcc phase of this isotope exists only over a very small temperature range near the melting curve.

I present in this work sound velocities measured in single crystals of bcc  $^4\text{He}$  whose quality and orientation were determined using x rays. The velocity data (at  $21.00\text{ cm}^3/\text{mole}$ ) are used to determine the elastic constants, mode Grüneisen parameters, the compressibility, and the Debye temperature. Comparisons are made with bcc  $^3\text{He}$  and with theoretical predictions.

Portions of this research have been reported, in preliminary form, elsewhere.<sup>19</sup>

### II. EXPERIMENTAL DETAILS

The apparatus and procedures used in this experiment, with a few exceptions, are the same as those described in detail in a previous publication.<sup>7</sup> The most significant modification in the apparatus has been the complete redesign of the freezing cell which will be described in Sec. IIA. In addition, the copper block which had been used to thermally anchor the fill capillary to the sample platform (at a point a few centimeters from the cell) was removed. Two changes were also made in the room-temperature gas-handling system (Fig. 4 of Ref. 7): The temperature-regu-

lated 100-cm<sup>3</sup> ballast volume was replaced with a 750-cm<sup>3</sup> volume, and a needle valve was placed in a new line joining valves 3 and 11. This valve made it possible to very precisely adjust the pressure at the beginning of the experiment. With the larger ballast volume, the pressure in the ballast-volume-cell system changed by less than 0.2% as a bcc  $^4\text{He}$  sample was grown. The pressure was monitored continuously on the Texas Instruments pressure gauge in the system which now contained a 0–68 bar metallic Bourdon tube. It was also necessary to modify the procedure followed in growing the helium crystals at constant pressure since the bcc  $^4\text{He}$  samples were grown from the superfluid liquid. These changes will be discussed in Sec. II D.

#### A. Freezing cell

Cross-sectional views of the freezing cell used in this work are shown in Fig. 1. The volume of the cell was 0.46 cm<sup>3</sup>; the volume between the ultrasonic transducers was 0.11 cm<sup>3</sup>. As with the cell used for the sound-velocity measurements in bcc  $^3\text{He}$ ,<sup>7</sup> the cell body was constructed of Plexiglass. However, the new cell had several advantages over the older design. With the quartz ultrasonic transducers mounted on the side walls of the cell, there were no significant obstructions to interfere with the growth of the crystals which could now be nucleated on a copper freezing tip. In addition there were no metal collars to reduce the region in which the diffracted-x-ray beam could be detected. The thickness of plastic in the beam path was cut by a factor of 2 in order to reduce the amount of background scattering.

The cell body was constructed by laminating three pieces of Plexiglass. The two end pieces were machined from a 0.32-cm-thick sheet and had windows for the x-ray beam which were 0.056 cm thick and approximately 0.64 cm in diameter. All tool marks on these windows were polished out, with care being taken during this process not to heat the plastic. After sand blasting all contact areas, the end pieces were epoxied<sup>20</sup> onto the

middle section of the laminant which was machined from a 0.64-cm-thick sheet. The slotted hole in this piece was 0.64 cm wide and 1.28 cm long. Stainless-steel wire springs (0.018 cm diam) were used to clamp the ultrasonic transducers (0.48 cm diam) against the flat walls of the cavity and to make the electrical ground connections to the transducers. The springs, the active electrical leads soldered to the back side of the transducers, the copper freezing tip (0.16 cm diam), and the copper capillary feed through were all sealed into the plastic cell body with epoxy.<sup>20</sup> The thermometers and heaters were mounted on copper blocks which were clamped onto the freezing-tip and capillary-feed-through rods. In addition a heater was wound on the 60-cm-long, 0.005-cm-i. d., 0.015-cm-o. d. stainless-steel filling capillary.

#### B. Sound-velocity measurements

The longitudinal and transverse sound velocities were measured in two different cells using a pulse echo technique. The two cells were identical except that cell 1 contained a pair of 5-mm-diam, 10-MHz shear (*AC*-cut quartz) ultrasonic transducers while cell 2 had 10-MHz compressional (*X*-cut quartz) transducers. The *longitudinal* velocities in bcc  $^4\text{He}$  measured with both sets of transducers agreed within the precision of the measurements. For this comparison the ultrasonic path lengths (nominally 0.6 cm) measured at room temperature were used. Because of possible small distortions of the cells under pressure the actual path lengths at low temperature were determined by multiplying the measured transit time in liquid  $^3\text{He}$  (using cell 2) by the corresponding sound velocity measured in a copper cell<sup>21</sup> with a nominal path length of 2 cm. It is estimated that the sound velocities are accurate to better than 0.5%.

A check on the path-length determination was made by measuring several shear velocities in hcp  $^4\text{He}$  crystals at 21.03 cm<sup>3</sup>/mole. These data are in excellent agreement (1%) with the results of Crepeau, Heybey, and Lee.<sup>11</sup>

The liquid  $^3\text{He}$  sound velocities at 1 K and at pressures between 10 and 40 bar measured in the copper cell were found to be about 0.7% larger than those reported by Vignos and Fairbank.<sup>22</sup> In my recently reported work on bcc  $^3\text{He}$ ,<sup>7</sup> their data had been used in determining the low-temperature ultrasonic path length. An additional 0.3% systematic error in my work has also been detected. The bcc  $^3\text{He}$  sound velocities reported in Ref. 7 should thus be increased by 1%.

Since I will be comparing the bcc  $^4\text{He}$  and  $^3\text{He}$  sound velocities, it is desirable to eliminate, as much as possible, systematic errors between the various sets of velocity data measured using dif-

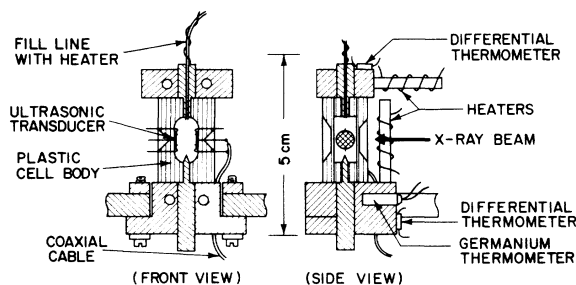


FIG. 1. Front- and side-cross-sectional views of the freezing cell.

ferent apparatuses and at different times. I therefore decided to also check my older<sup>6</sup> bcc <sup>3</sup>He data at 21.66 cm<sup>3</sup>/mole. Unfortunately, during the process of increasing the pressure, cell 2 burst at 42 bar. It was thus necessary to construct a new freezing cell.<sup>23</sup> The new cell withstood much higher pressures. Six longitudinal and one fast transverse velocities were measured in crystals of <sup>3</sup>He at 65.83 bar. These measurements are in excellent agreement with those previously reported.<sup>6</sup>

Changes in the sound velocity of bcc <sup>4</sup>He with temperature were measured by monitoring with an oscilloscope a particular cycle in one of the unrectified received ultrasonic pulses. A change in transit time of 2 nsec could be observed. This corresponds to a precision in these measurements of about one part in 10<sup>4</sup>.

### C. Procedure

Owing to (i) the extremely large effective thermal conductivity of the superfluid in the filling capillary,<sup>24</sup> (ii) the very small thermal conductivity of bcc <sup>4</sup>He,<sup>25</sup> and (iii) the very narrow temperature range over which the bcc phase of <sup>4</sup>He exists (see Fig. 2), the procedure that had been followed in growing bcc <sup>3</sup>He crystals<sup>7</sup> at constant pressure had to be modified considerably. If the heat leak down the capillary was larger than 20 μW, the cell could not be filled with solid. It was possible to reduce this heat leak to approximately 10 μW by using a long length (60 cm) of very small inside-diameter (0.005 cm) capillary with the

warm end of the capillary kept at a temperature less than 10 mK above the freezing temperature  $T_f$  of the solid.

The first sample of each run was grown according to the following procedure: With the cell temperature a few millidegrees above  $T_f$ , the pressure in the system was adjusted to 28.00 bar. The valve leading to the <sup>4</sup>He supply cylinder was then closed, leaving the cell connected only to the 750 cm<sup>3</sup> ballast volume and to the pressure gauge for the remainder of the run. The temperature measured at the cell bottom  $T_b$  was then lowered to and regulated at a temperature a few millidegrees above the bcc-hcp transition. During this process the temperature at the warm end of the capillary was kept considerably above  $T_f$ . The temperature measured at the top of the cell  $T_t$  was thus at  $T_f$ , and the differential thermometer read  $T_b - T_t \approx -40$  mK. The temperature at the warm end of the capillary was then gradually lowered in small steps until the capillary was blocked with solid, greatly reducing the heat leak to the cell. This was indicated when the differential thermometer suddenly started heading towards a zero gradient reading. With a previous calibration of the capillary thermometer normalized using this calibration point, the temperature at the warm end of the capillary could be accurately warmed a few millidegrees above  $T_f$  and kept at this point until the crystal was complete. The completion of the crystal was indicated by a decrease in the temperature gradient along the cell. The sample was now confined to move along an isochore, the density of the sample being an average of the local densities which had been a function of position (and temperature) along the length of the cell just prior to the completion of the crystal growth. Subsequent crystals could now be grown in a very routine manner. The temperature of the warm end of the capillary determined the growth time which usually ranged between 30–90 min and for most samples was about 40 min.

The first several samples grown had different orientations, however later samples generally had very nearly the same orientation. Several modifications in the growing procedure were tried in attempts to change the orientation. Simply lowering  $T_b$  very quickly or very slowly below  $T_f$  had no effect on the orientation, nor did increasing the heat current flowing through the sample during nucleation. Some minor success resulted from quickly lowering  $T_b$  into the hcp phase and then warming back into the bcc phase while passing a large heat current ( $\sim 200$  μW) through the sample. (The heat switch was now fully closed. See Fig. 2, Ref. 7.) A portion of the small amount of solid surrounding the freezing point had thus undergone the transitions bcc

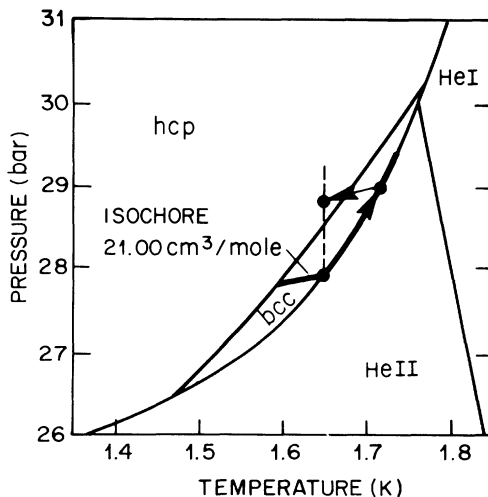


FIG. 2. Pressure-temperature phase diagram for bcc <sup>4</sup>He. The heavy curve indicates the path along which the temperature dependence of the sound velocities was measured. The arrows indicate schematically the procedure followed in relating the sound-velocity changes along the melting curve to changes of the velocities with molar volume at constant temperature.

– hcp – bcc. Warming the sample back into the bcc phase by increasing the heat flow through the cell also caused the seed to be partially melted back, hopefully leaving only solid which had undergone the two transitions. Crystals grown from seeds prepared in this manner did have more random orientations, but generally were of poorer quality, often being composed of many small crystallites with nearly the same orientations.

Before the second run, the polished, pointed freezing tip was ground down even with the plastic. This change did result in crystals growing with other orientations.

On the third run a new cell was used. The freezing tip in this cell was flat topped, but now with its surface polished. The crystals grown in this cell following the usual procedure tended to have nearly the same preferred orientation as those grown during the first run. It was found, however, that crystals of other orientations could be grown if the crystals were nucleated with essentially no heat flowing through the sample. This was accomplished by temporarily freezing a plug of solid in the capillary. Most of the crystals in this run were grown from seeds formed in this manner. The success in obtaining more randomly oriented bcc  $^4\text{He}$  crystals using this procedure may explain why the bcc  $^3\text{He}$  crystals grown previously<sup>7</sup> (but in a cell with a different geometry) had fairly random orientations. The heat leak down a liquid- $^3\text{He}$ -filled capillary is very small.

For several samples the temperature dependence of the sound velocity  $v$  was measured by slowly increasing or decreasing the temperature in 3–7 mdeg steps. Measurements of the changes in velocity along the melting curve could also be made since the liquid in the cell remained below the level of the transducers. It was thus possible to accurately determine the melting temperature  $T_m$  by noting the change in sign of  $\Delta v$ . These determinations of  $T_m$  varied a little from crystal to crystal indicating that the cell was not always completely filled with solid before the capillary was plugged. Nearly all samples for which  $T_m$  was determined had  $T_m = 1.655 \pm 0.010$  K. This corresponds<sup>17</sup> to a molar volume of  $21.00 \pm 0.01$  cm<sup>3</sup>.

### III. RESULTS AND DISCUSSION

#### A. Sound velocities

During the course of this work 123 bcc  $^4\text{He}$  crystals were grown at a molar volume of 21.00 cm<sup>3</sup>. The first 75 bcc samples were grown in cell 1 in which the shear ultrasonic transducers were mounted. Sound velocity-measurements could be made in only 26 of these 75 samples, and

only eight of these measurements corresponded to transverse velocities. In most of the remaining samples no signal or only an extremely weak longitudinal ultrasonic signal was observed. The fact that in most samples no transverse signal could be detected is understood since the energy-flux vectors associated with the two transverse waves can deviate substantially from the wave normal.<sup>26,27</sup> The longitudinal waves were excited and detected by the shear transducers since in anisotropic media the longitudinal (quasilongitudinal) displacement vector is generally not parallel to the wave normal. In cell 2, in which the compressional transducers were mounted, 48 crystals were grown; data were obtained for 35 of these samples. In total there were thus 61 data points corresponding to 53 longitudinal  $L$ , seven fast transverse  $T_1$ , and one slow transverse  $T_2$  sound-velocity measurements. These sound velocities, measured at 1.612 K, and the propagation directions ( $\theta$ ,  $\varphi$ ), determined using Laue transmission-x-ray photographs, are listed in Table I. The angles  $\theta$  and  $\varphi$  are defined in Fig. 3 where each of the propagation directions is plotted on a stereographic projection of  $\frac{1}{48}$ th of the reference sphere. The open and closed circles in the figure correspond, respectively, to propagation directions in which longitudinal and transverse velocities were measured (in cell 1) using shear transducers; the open squares correspond to directions in which the longitudinal velocities were measured (in cell 2) using compressional transducers. The "2" associated with some of the circles designates those crystals grown in cell 1 after the freezing tip in this cell was modified (see Sec. II C). The line segments drawn through all of the circles show the approximate displacement direction of the shear transducers relative to the major axes of each of the crystals. Since for many of these crystals the transducer-displacement directions have a large component parallel to the  $\{100\}$  plane, the slow transverse mode should have been the mode most strongly excited. A plot similar to Fig. 7(b) of Ref. 7 however shows that for most propagation directions the energy-flux vector for the  $T_2$  mode deviates from the propagation vector by such a large amount (greater than  $38^\circ$ ) that no portion of the beam will strike the opposite transducer without first being reflected by at least one wall of the cell. This means, due to the geometry of the cell, that in most cases a  $T_2$  signal could not be detected.

On five different occasions, apparent sound velocities of approximately 98 m/sec were measured for crystals oriented such that the propagation direction was in the (001) plane with  $(\theta, \varphi) \approx (38, 0)$  and such that the (001) plane was nearly perpendicular to the vertical axis of the cell. Since the

TABLE I. Sound velocities in bcc  ${}^4\text{He}$  at a molar volume of  $21.00 \text{ cm}^3$  and at  $1.612 \text{ K}$ . The angles  $\theta$  and  $\varphi$  are the spherical coordinates of the direction of sound propagation relative to the principal axes of the crystal. The calculated velocities are those determined by the three elastic constants (Eq. 4) resulting from a least-squares fit of all the data.

Mode	$\theta$ (degrees)	$\varphi$ (degrees)	Measured velocity (m/sec)	Calculated velocity (m/sec)	Relative difference
Longitudinal $L$	7	3	418	421.9	-0.010
	8	6	424	426.0	-0.006
	8	7	423	426.0	-0.006
	15	3	456	455.1	0.002
	18	4	467	466.6	0.001
	18	4	466	466.6	-0.002
	18	6	467	466.7	0.000
	20	32	480	478.0	0.003
	22	34	479	486.0	-0.015
	24	16	490	488.9	0.003
	26	7	494	492.9	0.001
	26	11	496	493.7	0.004
	28	42	503	508.1	-0.010
	31	16	505	508.3	-0.006
	31	16	508	508.3	-0.000
	31	44	517	517.4	-0.001
	32	20	514	512.4	0.003
	32	20	514	512.4	0.003
	32	23	515	513.9	0.002
	34	17	513	515.1	-0.004
	34	20	513	516.8	-0.007
	34	37	520	524.5	-0.008
	34	38	527	524.7	0.004
	35	7	515	512.3	0.005
	35	12	512	514.4	-0.004
	35	19	515	518.2	-0.006
	36	3	513	512.8	0.001
	36	8	514	514.2	0.000
	38	3	515	515.2	-0.000
	38	4	514	515.4	-0.002
	38	4	517	515.4	0.003
	38	6	514	516.0	-0.004
	38	12	525	518.7	0.012
	39	5	521	516.7	0.008
	39	8	521	517.8	0.006
	39	18	522	523.9	-0.004
	40	2	519	516.9	0.004
	40	8	521	518.7	0.005
	40	9	522	519.2	0.005
	40	10	521	519.7	0.003
	40	26	524	531.1	-0.014
	41	6	524	518.6	0.010
	41	7	522	519.0	0.006
	42	3	521	518.2	0.005
	42	16	527	525.6	0.003
	43	1	522	518.3	0.007
	45	14	519	525.7	-0.013
	46	17	520	528.8	-0.017
	46	33	548	543.1	0.008
	47	28	540	540.0	-0.000
	47	31	542	542.5	-0.001
	47	31	547	542.5	0.008
	48	34	542	545.3	-0.007

TABLE I. *Continued*

Mode	$\theta$ (degrees)	$\phi$ (degrees)	Measured velocity (m/sec)	Calculated velocity (m/sec)	Relative difference
Transverse $T_1$	9	17	337	336.1	0.002
	14	33	327	329.6	-0.008
	33	0	338	337.3	0.002
	35	7	334	334.5	-0.002
	38	3	340	336.7	0.009
	38	6	332	334.9	-0.009
	38	8	334	333.1	0.003
Transverse $T_2$	35	44	183	181.1	0.011

propagation vector lies in the (001) plane so does the energy-flux vector.<sup>26</sup> This means that the  $T_2$  beam should have struck the opposite transducer after being reflected from the nearly flat walls of the cell. After a reflection from a flat wall, the propagation vector is no longer perpendicular to the transducers, however the velocity component along the normal to the transducers is unchanged.<sup>26</sup> Thus if the pressure variations over the surface of the receiving transducer do not completely cancel, the first received ultrasonic pulse should correspond to the sound velocity with propagation vector normal to the transducers. The measured sound velocity of 98 m/sec is however about 15 m/sec slower than the velocity for this propagation direction calculated using the elastic constants determined by the sound velocities listed in Table I. This discrepancy is considerably larger than the  $\sim 5$  m/sec which corresponds to the estimated uncertainty in  $\theta$  of  $1^\circ$ . However the beam was actually not reflected by a flat wall, but instead by the thin-plastic x-ray windows which presumably were slightly bowed. This could account for the discrepancy. Unfortunately, the actual boundary conditions are unknown and so these  $T_2$  velocities could not be included in Table I nor used in determining the elastic constants. We believe though that they still do provide an important consistency check (10%) on the  $T_2$  velocity in the  $\langle 110 \rangle$  direction determined by the remainder of the velocity data, namely, 89 m/sec.

The present measurements on the  $L$  and  $T_1$  velocity surfaces can be compared with the sound velocities previously measured by others in samples of unknown crystal quality and with orientations not determined by direct measurement. The most meaningful comparison can be made with the shear velocity data of Lipschultz and Lee.<sup>28</sup> If their samples were single crystals these measurements must correspond to  $T_1$  velocities with propagation directions near the  $\{100\}$  plane.<sup>27</sup> In this region the  $T_1$  velocity is nearly constant.

Their measured shear velocities in the range 337–351 m/sec can thus be compared with the present determination of the  $T_1$  velocity with propagation vector lying in the  $\{100\}$  plane, namely,  $337 \pm 1$  m/sec. Both Vignos and Fairbank<sup>22</sup> and Lipschultz and Lee<sup>28</sup> measured longitudinal velocities near 535 m/sec. This velocity is consistent with the present results.

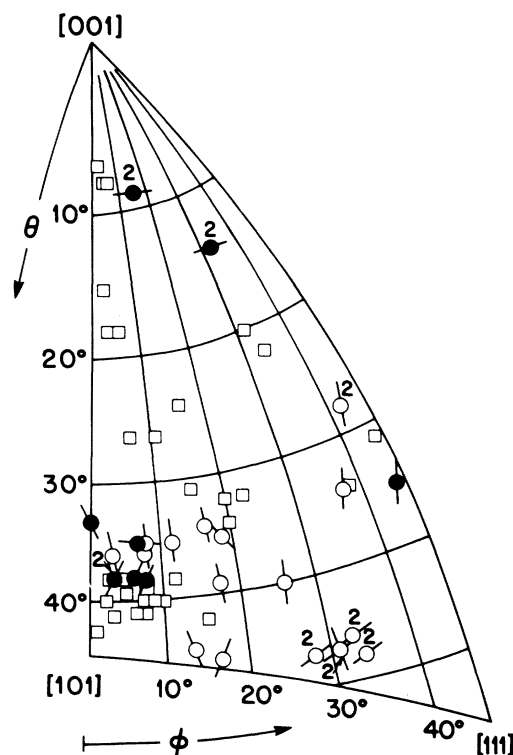


FIG. 3. Direction of wave propagation for each of the sound-velocity data points listed in Table I plotted on a stereographic projection of the unit triangle. The open and closed symbols correspond, respectively, to longitudinal and transverse sound-velocity measurements. Further details are given in the text.

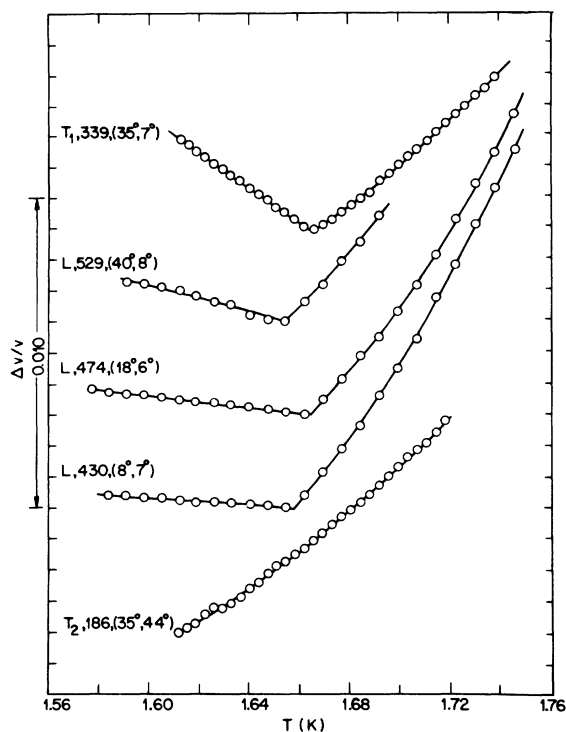


FIG. 4. Relative change in sound velocity as a function of temperature for five different crystals. Along the isochore the velocity is decreasing and along the melting curve the velocity is increasing with increasing temperature.

#### B. Molar volume dependence of the sound velocities

The temperature dependence of the sound velocities at constant density was measured for several crystals. In addition, measurements could also be made along the melting curve if the liquid portion of the sample was below the level of the transducers. The sound velocities decreased with increasing temperature when the crystal was kept at constant density and increased with increasing temperature along the melting curve. Thus it was possible to determine precisely at what temperature the melting curve was reached and consequently the molar volume of the isochore.<sup>17</sup> The relative change in the sound velocity  $[v(T) - v(T_0)]/v(T_0)$ , where  $T_0 = 1.612$  K is plotted as a function of temperature for several crystals in Fig. 4. Smooth curves have been drawn through the data points. The numbers associated with each of the curves are  $v(T_0)$  in m/sec and in parentheses the direction of wave propagation ( $\theta, \phi$ ). The different melting temperatures for the top four curves indicate the difficulty encountered in keeping the capillary open until a growing crystal completely filled the cell. The bottom curve in the figure corresponds to one of the first bcc samples grown and shows only

data on the melting curve indicating that in this case the melting temperature was less than  $T_0$  and thus that the capillary was plugged when a significant portion of the sample was liquid. Unfortunately, in an attempt to open the capillary and fill the remainder of the cell with solid, this crystal was completely melted and lost. The largest relative change in the velocity along an isochore was observed for the  $T_1$  mode where the velocity change was  $\sim 0.3\%$  between  $T_0$  and  $T_m = 1.666$  K. The small scatter in all of the data along the melting curve is presumably an indication that in the time interval (5–10 min) between measurements significant pressure gradients in the sample had relaxed.

Using both the isochoric data and the data along the melting curve, the molar volume dependence of the sound velocities at constant temperature was determined. For this calculation the plausible assumption was made that the temperature dependence of the sound velocities along isochores is independent of molar volume over the small molar volume range  $20.90$ – $21.00$   $\text{cm}^3$ . The procedure followed in relating the measured velocities to velocities along the desired path is indicated schematically by the arrows in Fig. 2. First, for each sound-velocity datum point of a given crystal, taken at a temperature  $T$  along the melting curve,  $v(T, V) - v(T_m, V_m)$  was determined. This change in velocity was then added to  $v(T_m, V) - v(T, V)$  along the isochore in order to obtain  $\Delta v \equiv v(T_m, V) - v(T_m, V_m)$ . The change in velocity along the isochore was taken to be equal to  $(T_m - T)(\partial v/\partial T)_V$  with  $(\partial v/\partial T)_V$  being determined for each sample using the slope of the straight line drawn through the isochoric data in Fig. 4. The molar volume was determined using the  $V$ - $T$  data along the melting curve of Hoffer.<sup>17</sup> The results are given in Fig. 5, where  $\Delta v$  is plotted as a function of molar volume ( $T \approx 1.66$  K). It should be noted that  $\Delta v$  was calculated for molar volumes extending down to  $20.90$   $\text{cm}^3$ , although in reality the bcc  $\rightarrow$  hcp transition prevents compressing the stable bcc solid at this temperature to molar volumes less than approximately  $20.94$   $\text{cm}^3$ . For all four curves, the data fall very nearly along straight lines with the magnitude of the slopes increasing with increasing velocity. The slopes were determined by a least-squares fitting of the data between  $20.95$  and  $21.00$   $\text{cm}^3/\text{mole}$  and were used, together with the relation

$$\gamma_m(T) = \frac{1}{3} - \frac{V}{v(T)} \left( \frac{\partial v}{\partial V} \right)_T \quad (1)$$

to calculate the mode Grüneisen parameter  $\gamma_m$ . For the  $T_1$  mode with velocity 339 m/sec we found  $\gamma_m = 2.74$ ; for the longitudinal modes with velocities 430, 474, and 529 m/sec, we found, respec-

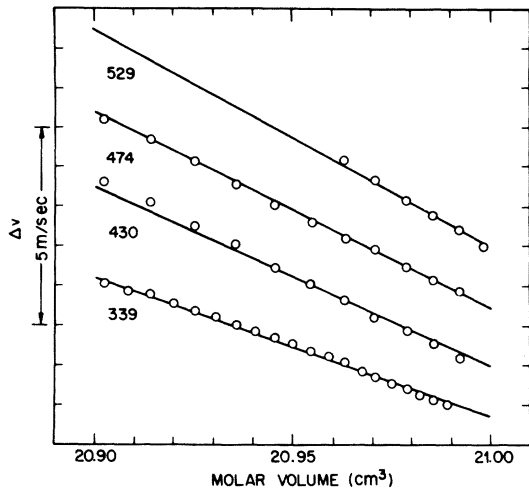


FIG. 5. Molar volume dependence of the sound velocities at constant temperature for four different samples determined using the corresponding isochore and melting-curve velocity data shown in Fig. 4. The numbers give the nominal velocities in m/sec.

tively, mode  $\gamma$ 's of 2.64, 2.39, and 2.71. The uncertainty in each of these values is estimated to be less than 0.2. In the figure, the straight lines drawn through each of the sets of data correspond to  $\gamma_m = 2.5$ . If, in a cubic system, the mode  $\gamma$ 's and the propagation directions corresponding to any three different sound velocities are precisely known, then the mode  $\gamma$  for sound propagating in any direction and hence  $\gamma^\epsilon(T) \equiv -[V/\Theta^\epsilon(T)](\partial\Theta^\epsilon/\partial V)_T$  can be calculated. Here  $\Theta^\epsilon(T)$  is the Debye temperature determined by the sound velocities measured at temperature  $T$ . However, if all three velocities are on the  $L$  and  $T_1$  velocity surfaces, then even small uncertainties in these mode  $\gamma$ 's imply very large uncertainties in the  $T_2$  mode  $\gamma$ 's, particularly for propagation near the  $\langle 110 \rangle$  direction. As a consequence  $\gamma^\epsilon(T)$  is also very uncertain. It is thus necessary to restrict the comparison with the bcc phase of  ${}^3\text{He}$  to the  $L$  and  $T_1$  velocity surfaces. In computing the  ${}^3\text{He}$  mode  $\gamma$ 's, the measured<sup>7</sup> elastic constants at 24.45 and 21.66 cm<sup>3</sup>/mole were used. (The constants at 24.45 cm<sup>3</sup>/mole were first corrected by 1%, see Sec. II B.) The  $\gamma_m$ 's, calculated assuming no molar volume dependence, are  $2.37 \pm 0.11$ ,  $2.65 \pm 0.10$ , and  $2.88 \pm 0.10$ , respectively, for  $L$  waves propagating in the  $\langle 100 \rangle$  and  $\langle 110 \rangle$  directions and for  $T_1$  waves with propagation vector in the  $\{100\}$  plane. These values are in line with the  ${}^4\text{He}$  results.

### C. Elastic constants

The three elastic constants were determined by a least-squares fitting of all of the velocity data listed in Table I. Each of the data points was

weighted by  $W = (\delta v)^{-2} \propto v^{-4} \delta t^{-2}$ . The total uncertainty  $\delta t$  in the transit time for sound propagating in direction  $(\theta, \varphi)$  was due to the uncertainty  $\delta t_i$  in the time interval measurement itself, which was taken to be 0.1  $\mu\text{sec}$  for all data, and also to the uncertainty in the propagation direction. Thus

$$\delta t = \delta t_i + \frac{t}{v} \frac{\partial v}{\partial \theta} \delta \theta + \frac{t}{v} \frac{\partial v}{\partial \varphi} \delta \varphi. \quad (2)$$

The derivatives of the velocities with respect to  $\theta$  and  $\varphi$  were roughly estimated from a grid of velocities calculated using preliminary estimates of the elastic constants. Both  $\delta \theta$  and  $\delta \varphi$  were taken to be  $1^\circ$ . The following are the weights actually applied to the data:

$$\begin{aligned} W_L &= 1 & \text{for } \theta \leq 30^\circ, \\ W_L &= 2 & \text{for } \theta > 30^\circ, \\ W_{T_2} &= 5 & \text{for } \theta, \varphi = 35^\circ, 44^\circ, \\ W_{T_1} &= 10 & \text{for all } T_1 \text{ data.} \end{aligned} \quad (3)$$

The best-fit reduced elastic constants for<sup>29</sup> bcc  ${}^4\text{He}$  at  $T = 1.612$  K are

$$\begin{aligned} C_{11}/\rho &= 1.630 \pm 0.005, & C_{12}/\rho &= 1.473 \pm 0.007, \\ C_{44}/\rho &= 1.137 \pm 0.003, \\ (C_{11} - C_{12})/2\rho &= 0.079 \pm 0.005, \end{aligned} \quad (4)$$

where the units are  $10^5 \text{ m}^2/\text{sec}^2$  and where  $\rho$  is the density. The uncertainties quoted are standard errors in the parameters which were determined with account being taken of correlations between the parameters. A refitting of the data with the weight function set equal to unity yielded elastic constants not significantly different from those quoted above, however the standard errors computed were considerably larger. The effects of a systematic error in the propagation direction were determined by a refitting of the data with both  $\theta$  and  $\varphi$  increased by  $1^\circ$ . If we allow for this possible systematic error then the uncertainty in the moduli given in Eq. (4) are increased, respectively, to  $\pm 0.036$ ,  $\pm 0.034$ ,  $\pm 0.010$ , and  $\pm 0.008$ .<sup>30</sup>

The present elastic constants are consistent with those determined by Osgood *et al.*<sup>10</sup> from neutron scattering data ( $C_{11}/\rho = 1.77 \pm 0.32$ ,  $C_{12}/\rho = 1.58 \pm 0.35$ , and  $C_{44}/\rho = 1.07 \pm 0.10$ ). The moduli inferred by Wanner<sup>27</sup> from an analysis of transverse sound velocity, compressibility, and specific-heat data ( $C_{11}/\rho = 1.73 \pm 0.26$ ,  $C_{12}/\rho = 1.52 \pm 0.26$ , and  $C_{44}/\rho = 1.23 \pm 0.05$ ) are in fair agreement with those given in Eq. (4) however the difference between the two values of  $C_{44}/\rho$  is larger than the combined quoted uncertainties.

In a classical harmonic solid, the sound velocities are inversely proportional to the square root of the mass of the atoms. Thus for two clas-



sical crystals which differ only in the mass of the atoms,  $v_1/v_2 = (m_2/m_1)^{1/2}$ , where  $v_1$  and  $v_2$  are any two corresponding velocities in the two systems. It then follows that the ratio  ${}^1\Theta_0/{}^2\Theta_0$  of the Debye temperature at 0 K must also equal  $(m_2/m_1)^{1/2}$ . Solid  ${}^3\text{He}$  and  ${}^4\text{He}$  are certainly not classical crystals, but on the other hand, in many respects they do behave quite surprisingly like classical solids, and so it is interesting to pursue this type of comparison between the two isotopes. It might be noted first that in the hcp phases of  ${}^3\text{He}$  and  ${}^4\text{He}$ , specific-heat measurements<sup>3,4</sup> indicate  ${}^3\Theta_0/{}^4\Theta_0 \approx 1.18$  for molar volumes between 11.4 and 19.0  $\text{cm}^3$ . In addition, recent measurements of the optic-mode frequencies at the zone center in the two isotopes also yield a ratio of 1.18.<sup>31</sup> These experimental results are only slightly larger than the classical value  $\sqrt{3/2} = 1.155$ . Unfortunately there have been no sound-velocity measurements in hcp  ${}^3\text{He}$  crystals of known orientation and so it is not possible to make the more detailed comparison of the corresponding sound velocities.

In the bcc phases of helium, the comparison of the calorimetric Debye temperatures cannot be made since it is not possible to accurately determine  $\Theta_0$  from the specific-heat measurements for either isotope. In  ${}^4\text{He}$ , the bcc phase does not exist at very low temperatures. In  ${}^3\text{He}$ , there is an anomaly in the low-temperature specific heat. A comparison can be made using  $\Theta_0$ 's determined from sound-velocity data. However these measurements permit the more detailed and more revealing comparison of the sound velocities themselves. Sound velocities in oriented crystals have not been measured in the two isotopes at precisely the same molar volume. It was thus necessary first to extrapolate the  ${}^3\text{He}$  results at larger molar volumes to 21.00  $\text{cm}^3/\text{mole}$  assuming that the mode Grüneisen parameter

$$\gamma_{ij} = -\frac{1}{2} \frac{d \ln C_{ij}}{d \ln V} - \frac{1}{6} \quad (5)$$

is independent of molar volume. The calculated ratios of the  ${}^3\text{He}$ -to- ${}^4\text{He}$  sound velocities in the  $\langle 100 \rangle$  direction for the  $L$ ,  $T_1$ , and  $T_2$  modes are, respectively, 1.38, 1.21, and 1.21. The ratios in the  $\langle 110 \rangle$  direction are 1.31, 1.21, and 1.24, and in the  $\langle 111 \rangle$  direction are 1.30, 1.20, and 1.20. The longitudinal ratios are considerably larger than the classical value of 1.155. However, all of these values are in excellent agreement with the respective ratios implied by the quantum-mechanical sound-velocity calculations of Horner.<sup>32</sup>

A graphical comparison of the  ${}^3\text{He}$  and  ${}^4\text{He}$  sound velocities for propagation directions in the symmetry planes is made in Fig. 6(a). The solid

curves in this figure correspond to the sound velocities in bcc  ${}^4\text{He}$ . The dashed curves are the  ${}^3\text{He}$  sound velocities scaled by  $(3/4)^{1/2}$ . Thus, if the two solids were simple harmonic solids, the two sets of curves would coincide. Since the low-temperature specific heat is dominated by the *transverse* modes, a comparison of the Debye temperatures for the two isotopes ( ${}^3\Theta_0/{}^4\Theta_0 = 1.24 \pm 0.11$ ) does not reflect the large deviations from classical behavior in the *longitudinal* modes. It is thus possible that the hcp phases may also be more nonclassical than the calorimetric data along suggest.

The isotopic ratios of the elastic constants themselves are listed in Table II. For classical solids the two sets of moduli would be identical, i. e., each of the three ratios would be equal to

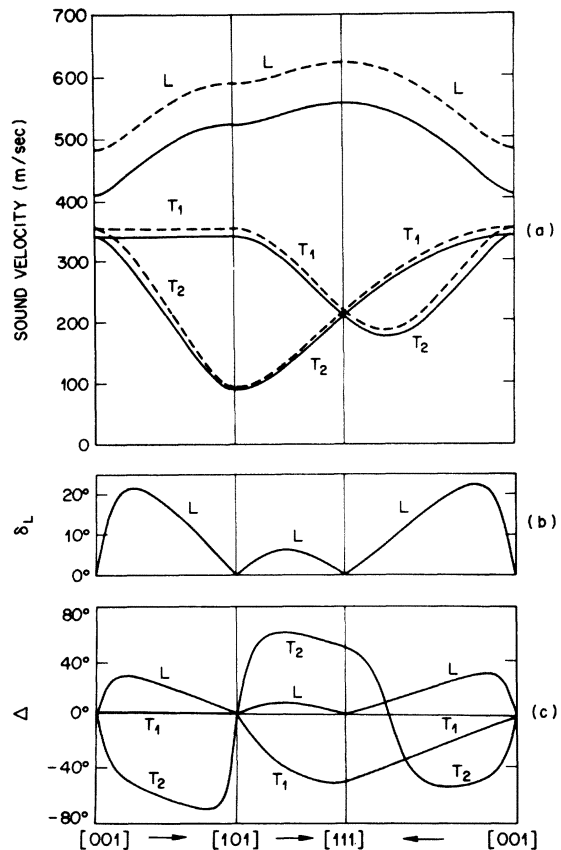


FIG. 6. (a) Longitudinal and transverse sound velocities; (b) deviation of the quasilongitudinal displacement vector from the wave normal; and (c) deviations of the sound rays from the wave normal, plotted for wave propagation vectors lying in the cubic symmetry planes. The curves were calculated using the elastic constants of bcc  ${}^4\text{He}$  at 21.00  $\text{cm}^3/\text{mole}$  given in Eq. (4). The arrows indicate the sense of positive deviations. The dashed curves are the  ${}^3\text{He}$  sound velocities at the same molar volume scaled by  $\sqrt{3/4}$ . If bcc  ${}^3\text{He}$  and  ${}^4\text{He}$  were classical solids the two sets of curves would coincide.

TABLE II. Comparison of bcc  $^3\text{He}$  and  $^4\text{He}$  elastic constants  $^3C_{ij}$ ,  $^4C_{ij}$ , and mode Grüneisen parameters  $^3\gamma_{ij}$ ,  $^4\gamma_{ij}$ , at 21.00 cm<sup>3</sup>/mole. The moduli are in units of  $10^8$  dyn/cm<sup>2</sup>.

	Experiment	Theory Horner (Ref. 32)	Theory Glyde & Goldman (Ref. 33)
$^3C_{11}$	4.447 ± 0.076	4.35	
$^3\gamma_{11}$	2.37 ± 0.11	2.37	
$^3C_{12}$	4.13 ± 0.16	3.42	
$^3\gamma_{12}$	2.74 ± 0.21	2.63	
$^3C_{44}$	2.393 ± 0.031	2.78	
$^3\gamma_{44}$	2.88 ± 0.10	2.30	
$^4C_{11}$	3.108 ± 3.02	3.02	
$^4\gamma_{11}$	2.5 ± 0.2	...	
$^4C_{12}$	2.810 ± 0.065	2.26	
$^4\gamma_{12}$	...	...	
$^4C_{44}$	2.167 ± 0.019	2.43	
$^4\gamma_{44}$	2.7 ± 0.2	...	
$^3C_{11}/^4C_{11}$	1.43 ± 0.06	1.44	1.54
$^3C_{12}/^4C_{12}$	1.47 ± 0.09	1.51	1.67
$^3C_{44}/^4C_{44}$	1.10 ± 0.03	1.14	0.95

unity. Given in the table, in addition to the theoretical isotopic ratios determined using the sound velocities tabulated by Horner,<sup>32</sup> are ratios calculated by Glyde and Goldman.<sup>33</sup>

Plotted in Figs. 6(b) and 6(c) are the deviations  $\delta_L$  of the quasilongitudinal displacement vector from the wave normal and the deviations  $\Delta$  of the sound rays from the wave normal,<sup>26</sup> computed using the  $^4\text{He}$  elastic constants given in Eq. (4). These figures can be compared with the corresponding figures computed for bcc  $^3\text{He}$  at 24.45 cm<sup>3</sup>/mole (Figs. 8(b) and 8(c) of Ref. 7) and with curves computed for  $^3\text{He}$  at 21.00 cm<sup>3</sup>/mole. At the same molar volume the  $\Delta$ 's are not significantly different but the maximum value of  $\delta_L$  is only 15° in  $^3\text{He}$ , whereas in  $^4\text{He}$   $\delta$  can be as large as 22°.

#### D. Compressibility

The adiabatic volume compressibility was determined using the expression

$$\beta_v^s = 3/(C_{11} + 2C_{12}), \quad (6)$$

with the results  $\beta_v^s = (3.437 \pm 0.072) \times 10^{-3}$  bar<sup>-1</sup>. This value and the thermodynamic relation

$$\beta_v^T \approx \beta_v^s + \alpha^2 VT/C_v \quad (7)$$

were then used to compute the *isothermal* compressibility  $\beta_v^T$ . Values of the expansion coefficient  $\alpha$  and of the constant volume specific heat  $C_v$  were taken from the tables given by Hoffer.<sup>17</sup> The calculated compressibility  $\beta_v^T = 3.64 \times 10^{-3}$  bar<sup>-1</sup> is in satisfactory agreement with the less

certain values determined by others<sup>15-17,34</sup> from thermodynamic measurements.

#### E. Debye temperature

Using the elastic constants given in Eq. (4), the elastic Debye temperature  $\Theta^e$  was determined by numerical integration. This calculation yielded the result  $\Theta^e = 19.17 \pm 0.50$  K at  $T = 1.612$  K. The stated uncertainty in this value is due both to random errors and to the possible systematic errors in the crystal orientation. It was determined by simultaneously adjusting the elastic constants within their error limits to give the maximum and minimum values of  $\Theta^e$ .

Based on the observed<sup>35</sup> temperature dependence of the sound velocities in bcc  $^3\text{He}$ , one would expect that if the bcc phase of  $^4\text{He}$  were also stable down to absolute zero,  $\Theta^e(0 \text{ K}) \equiv \Theta_0$  would be very nearly equal to the elastic Debye temperature measured near the melting curve. The estimate of  $\Theta_0$  can be made more precise. All of the measurements of the temperature dependence of the  $^4\text{He}$  sound velocities showed that the isochoric velocities increased with decreasing temperature. The same behavior was also observed for the slow transverse ( $T_2$ ) signals which were reflected from the cell walls (Sec. III A). Thus  $\Theta_0 > \Theta^e(1.6 \text{ K})$ . In bcc  $^3\text{He}$  at 24.1 cm<sup>3</sup>/mole, Wanner *et al.*<sup>35</sup> found that the change in velocity for all modes between 123 mK and the melting temperature could be well described by the function

$$v^2(T) - v^2(0) = -AT^4 - BT^6. \quad (8)$$

We have assumed that the same functional form would also describe the  $^4\text{He}$  data. It is not possible though to determine  $A$ ,  $B$ , and  $v(0)$  since the  $v(T)$  data extend over such a small temperature range. However, an upper limit for  $v(0)$  can be computed using  $v$  and  $dv/dT$  measured near the melting curve and Eq. (8) with  $B$  set equal to zero. Referring to the data shown in Fig. 4, I found  $[v(1.612 \text{ K}) - v(0)]/v(1.612 \text{ K})$  for the  $T_1$  mode to be less than 2% and for each of the longitudinal velocities less than 1%. I also computed the relative velocity change for the slow  $T_2$  mode propagating near the  $\langle 110 \rangle$  direction (see Sec. III A). In this case,  $\Delta v/v < 0.03\%$ . These results were used to modify the elastic constants given in Eq. (4) which were then in turn used to compute an upper limit of  $\Theta_0$ . This upper limit was found to be approximately 1% larger than  $\Theta^e(1.612 \text{ K})$ . Thus to within 1%,  $\Theta_0 = \Theta^e(1.612 \text{ K})$ . This value can be compared with the necessarily rough estimates of  $\Theta_0$  made by others based on measurements of the specific heat near the melting curve. Ahlers<sup>14</sup> estimated  $\Theta_0$  to be between 18.4 and 19.9 K. Edwards and Pandorf<sup>16</sup> and Hoffer<sup>17</sup> estimated values of 21.0 and 22.4 K, respectively.

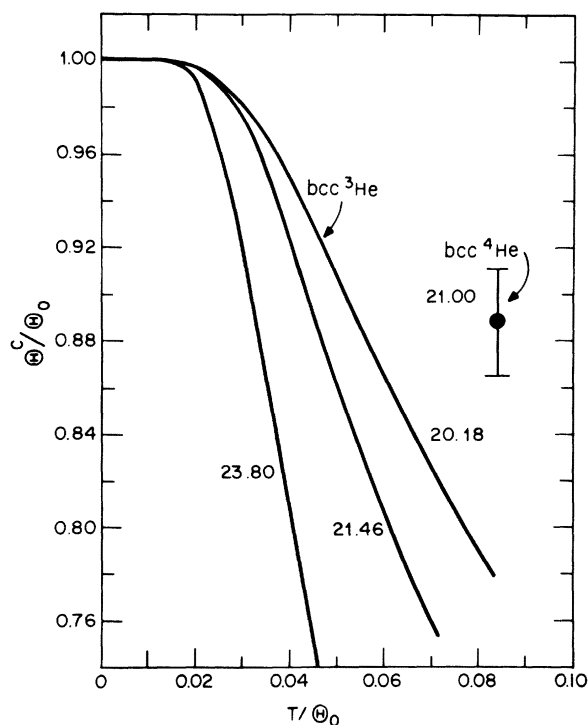


FIG. 7. Reduced Debye  $\Theta$  versus temperature plot. The three curves for bcc  $^3\text{He}$  were determined solely from calorimetric data assuming  $^3\Theta_0 = ^3\Theta^{\text{max}}$  (Ref. 3). The point for bcc  $^4\text{He}$  was determined using the calorimetric data (Refs. 14–17) and  $^4\Theta_0 = ^4\Theta^c(1.612 \text{ K})$ . The numbers give the molar volume in  $\text{cm}^3$ .

The calorimetric Debye temperature of bcc  $^4\text{He}$ ,  $^4\Theta^c$ , at 1.6 K is 17.0 K.<sup>14–17</sup> Thus,  $^4\Theta^c/^4\Theta_0 \approx ^4\Theta^c/^4\Theta^e = 0.88 \pm 0.03$  for  $T/^4\Theta_0 = 0.083$ . As shown in Fig. 7, this point lies considerably above the reduced curves for bcc  $^3\text{He}$  determined by Sample and Swenson,<sup>3</sup> assuming that the maximum value  $^3\Theta^{\text{max}}$  of  $^3\Theta^c(T)$  (occurring at  $T \approx 0.5 \text{ K}$ ) is equal to  $^3\Theta_0$ . The large molar volume dependence of the reduced  $^3\text{He}$  curves is generally attributed to a contribution to the specific heat owing to thermally activated vacancies.<sup>36</sup> According to the model of deWette,<sup>37</sup> the vacancy contribution to the specific heat of bcc  $^4\text{He}$  should be relatively larger than in bcc  $^3\text{He}$  since a larger compressibility corresponds to a lower vacancy activation energy. Thus one might have expected the  $^4\text{He}$  reduced Debye temperature to have fallen below the  $^3\text{He}$  curve at the same molar volume. The large discrepancy suggests that perhaps the assumption  $^3\Theta_0 = ^3\Theta^{\text{max}}$  is incorrect (at least for molar volumes near  $21.00 \text{ cm}^3$ ) and that we are comparing different quantities in  $^3\text{He}$  and in  $^4\text{He}$ . Indeed, sound-velocity measurements<sup>6,7</sup> in bcc  $^3\text{He}$  at  $21.66 \text{ cm}^3/\text{mole}$  yield a value<sup>30</sup> of  $^3\Theta_0$  which is  $(9 \pm 4)\%$  less than the corresponding  $^3\Theta^{\text{max}}$ . If the reduced calorimetric Debye temperature of bcc

$^4\text{He}$  is redetermined using in place of  $^4\Theta^e$ , a value which is roughly 10% larger, then the new reduced Debye temperature falls on the corresponding  $^3\text{He}$  curve. It is possible then, that if the bcc phase of  $^4\text{He}$  were stable down to absolute zero, specific-heat measurements on this isotope would also yield a maximum Debye temperature which is about 10% larger than the elastically determined zero-temperature Debye  $\Theta$ . The differences between  $\Theta^{\text{max}}$  and  $\Theta_0$  for both  $^3\text{He}$  and  $^4\text{He}$  could be explained by an anomalous, upward-curving phonon dispersion.<sup>32,38</sup> However, to reconcile this with the recent elastic measurements on bcc  $^3\text{He}$  at  $24.45 \text{ cm}^3/\text{mole}$ , where it was observed that  $^3\Theta^e \approx ^3\Theta^{\text{max}}$ , it would be necessary to conclude that the phonon dispersion of  $^3\text{He}$  must be essentially normal at very large molar volumes and becomes more anomalous with increasing density. Relating to this speculation it is interesting to note that in  $^3\text{He}$  at  $24.45 \text{ cm}^3/\text{mole}$  the anisotropy ratio  $A \equiv 2C_{44}/(C_{11} - C_{12})$  is equal to  $5.5 \pm 0.5$ , while at  $21.66 \text{ cm}^3/\text{mole}$   $A$  has grown to  $11.4 \pm 2.6$ . The ratio in bcc  $^4\text{He}$  at  $21.00 \text{ cm}^3/\text{mole}$  is  $14.4 \pm 2.2$ . The phonon spectra calculated by Horner<sup>32</sup> show anomalous dispersion and at molar volumes near  $21.55 \text{ cm}^3$  imply a difference between  $^3\Theta_0$  and  $^3\Theta^{\text{max}}$  close to that experimentally observed. The difference between the two theoretical Debye temperatures is however, essentially constant for molar volumes between  $20.18$  and  $23.80 \text{ cm}^3$ .

#### F. Premelting effect

Hoffer<sup>17</sup> and Alder *et al.*<sup>18</sup> have reported a pre-transition anomaly in the specific heat of bcc  $^4\text{He}$  near melting. Beginning approximately 20 mK below the melting temperature, their reported specific heat rises very rapidly before jumping discontinuously at the melting temperature to its value in the solid-liquid two-phase region. These authors concluded that this behavior was a characteristic of the melting process. An effect similar to this has also been observed by Edwards and Pandorf.<sup>16</sup> However, here the effect was attributed to density gradients in the helium samples which were contained in a cell filled with sintered copper powder. Measurements of the specific heat by Ahlers<sup>14,15,39</sup> showed no evidence of the anomalous contribution.

Within the precision of the present sound-velocity data I also saw no precursor to melting. In none of the curves shown in Fig. 5 is there any change in the temperature dependence of the sound velocities as the melting temperature is approached. However, it is the very slow transverse mode in the  $\langle 110 \rangle$  direction which one would expect to be most sensitive to the onset of melting. As discussed in Sec. III A, I believe I have observed  $T_2$  signals with propagation directions

near  $\langle 110 \rangle$ . Although, as noted, the sound rays associated with these modes were reflected by the bowed x-ray windows of the cell before striking the receiving ultrasonic transducer. This prevented the accurate determination of both the sound velocity itself and of the temperature dependence of the velocity. Nonetheless, if there had been any significant change in the real velocity of this mode it should have been detected. What was observed is that the apparent velocity was linear in temperature over the whole width of the phase.

I was not able to make accurate measurements of the temperature dependence of the ultrasonic attenuation, owing to very nonreproducible behavior. In no instance, however, did I observe any dramatic change in the attenuation near the melting temperature. In fact, all of the signals observed directly along the melting curve were nearly as intense as those observed considerably below the melting temperature.

#### IV. SUMMARY

Single crystals of bcc  $^4\text{He}$  of very high quality were grown under constant pressure from the superfluid in a plexiglass cell. The design of the cell permitted an x-ray examination of the samples and also allowed longitudinal and transverse sound velocities to be measured. The sound-

velocity data are in general agreement with measurements by others in samples of unknown orientation. Measurements of the temperature dependence of the velocities along an isochore and along the melting curve permitted determinations of several mode Grüneisen parameters. Within their uncertainties these parameters are in agreement with those obtained for bcc  $^3\text{He}$ . A weighted least-squares fitting of all of the velocity data at 1.612 K was used to determine the three elastic constants. A comparison of these constants with those of bcc  $^3\text{He}$  at the same molar volume showed that the isotopic ratios  $^3C_{ij}/^4C_{ij}$  of the moduli (particularly for  $C_{11}$  and  $C_{12}$ ) are considerably larger than the classical ratio of unity. The ratios are however in excellent agreement with the theory of Horner. The elastic constants were used to determine the compressibility and the Debye temperature. The Debye temperature was compared with existing calorimetric data. Within the precision of the sound velocity measurements no evidence at all of any premelting phenomena was observed.

#### ACKNOWLEDGMENTS

I am grateful to G. Ahlers and L. R. Testardi for several helpful discussions and for commenting on a manuscript of this paper.

- <sup>1</sup>L. H. Nosanow, Phys. Rev. **146** 120 (1966).  
<sup>2</sup>J. Wilks, *The Properties of Liquid and Solid Helium* (Clarendon, Oxford, 1967).  
<sup>3</sup>H. H. Sample and C. A. Swenson, Phys. Rev. **158**, 188 (1967).  
<sup>4</sup>G. Ahlers, Phys. Rev. A **2**, 1505 (1970).  
<sup>5</sup>N. R. Werthamer, Am. J. Phys. **37**, 763 (1969).  
<sup>6</sup>D. S. Greywall, Phys. Rev. A **3**, 2106 (1971).  
<sup>7</sup>D. S. Greywall, Phys. Rev. B **11**, 1070 (1975).  
<sup>8</sup>V. J. Minkiewicz, T. A. Kitchens, F. P. Lipschultz, and G. Shirane, Phys. Rev. **174**, 267 (1968).  
<sup>9</sup>R. A. Reese, S. K. Sinha, T. O. Brun, and C. R. Tilford, Phys. Rev. A **3**, 1688 (1971).  
<sup>10</sup>E. B. Osgood, V. J. Minkiewicz, T. A. Kitchens, and G. Shirane, Phys. Rev. A **5**, 1537 (1972).  
<sup>11</sup>R. H. Crepeau, O. Heybey, D. M. Lee, and S. A. Strauss, Phys. Rev. A **3**, 1162 (1971).  
<sup>12</sup>R. C. Pandorf and D. O. Edwards, Phys. Rev. **169**, 222 (1968).  
<sup>13</sup>S. H. Castles and E. D. Adams, Phys. Rev. Lett. **30**, 1125 (1973).  
<sup>14</sup>G. Ahlers, Phys. Rev. Lett. **10**, 439 (1963).  
<sup>15</sup>G. Ahlers, Phys. Rev. **135**, A 10 (1964).  
<sup>16</sup>D. O. Edwards and R. C. Pandorf, Phys. Rev. **144**, 143 (1966).  
<sup>17</sup>J. K. Hoffer, Ph. D. thesis (University of California, 1968) (unpublished).  
<sup>18</sup>B. J. Alder, W. R. Gardner, J. K. Hoffer, N. E. Phillips, and D. A. Young, Phys. Rev. Lett. **21**, 732 (1968).  
<sup>19</sup>D. S. Greywall, in *Proceedings of the Fourteenth International Conference on Low-Temperature Physics* (Otaniemi, Finland, 1975, edited by M. Krusius and M. Vuorio (North-Holland, Amsterdam, 1975), Vol. 1, p. 483).  
<sup>20</sup>1266, Emerson and Cummings, Inc., Canton, Mass.  
<sup>21</sup>The plastic cell body of the freezing cell described in Ref. 7 was replaced with a longer copper body for these measurements.  
<sup>22</sup>J. H. Vignos and H. A. Fairbank, Phys. Rev. **147**, 185 (1966).  
<sup>23</sup>The window pieces of the laminant (see Fig. 1) were machined round, concentric with the window, and epoxied into counter-bored holes in the body piece, which was now made from 1.27-cm-thick plastic. One shear and one compressional transducer were mounted in the cell.  
<sup>24</sup>B. Bertman and T. A. Kitchens, Cryogenics **8**, 36 (1968).  
<sup>25</sup>B. Bertman, H. A. Fairbank, C. W. White, and M. Crooks, Phys. Rev. **142**, 74 (1966); R. Berman and S. J. Rogers, Phys. Lett. **9**, 115 (1964).  
<sup>26</sup>G. F. Miller and M. J. Musgrave, Proc. R. Soc. Lond. **236**, 352 (1956); M. J. P. Musgrave, Rep. Prog. Phys. **22**, 74 (1959).  
<sup>27</sup>R. Wanner, Phys. Rev. A **3**, 448 (1971).  
<sup>28</sup>F. P. Lipschultz and D. M. Lee, Phys. Rev. Lett. **14**, 1017 (1965).  
<sup>29</sup>These elastic constants are smaller than those reported in a preliminary publication (Ref. 18). The difference corresponds to a more accurate determination of the low-temperature ultrasonic path length (see Sec. II (B)).  
<sup>30</sup>Our previously published elastic constants for bcc  $^3\text{He}$  (Refs. 6, 7) were determined by a least-squares fitting of the data with the weight function set equal to unity.

In addition no account was taken of the possible systematic errors in the orientations of the samples. An analysis, identical to that performed on the  $^4\text{He}$  data, which corrects these deficiencies yielded the following moduli. At  $24.45 \text{ cm}^3/\text{mole}$ :  $C_{11}/\rho = 1.664 \pm 0.024$ ,  $C_{12}/\rho = 1.384 \pm 0.033$ ,  $C_{44}/\rho = 0.768 \pm 0.007$ ,  $(C_{11} - C_{12})/2\rho = 0.140 \pm 0.010$ . At  $21.66 \text{ cm}^3/\text{mole}$ :  $C_{11}/\rho = 2.726 \pm 0.031$ ,  $C_{12}/\rho = 2.476 \pm 0.063$ ,  $C_{44}/\rho = 1.423 \pm 0.013$ ,  $(C_{11} - C_{12})/2\rho = 0.125 \pm 0.023$ . The moduli at the larger molar volume have also been increased by 2% relative to the previously published results corresponding to a 1% correction of the ultrasonic path length (see Sec. II B). These constants imply Debye temperatures of  $18.66 \pm 0.34 \text{ K}$  and  $22.60 \pm 0.97 \text{ K}$ , respectively.

<sup>31</sup>R. E. Slusher and C. M. Surko (unpublished)

<sup>32</sup>H. Horner, *J. Low Temp. Phys.* **8**, 511 (1972).

- <sup>33</sup>H. R. Glyde and V. V. Goldman (private communication).
- <sup>34</sup>E. R. Grilly, *J. Low Temp. Phys.* **11**, 33 (1973).
- <sup>35</sup>R. Wanner, K. H. Mueller, Jr., and H. A. Fairbank, *J. Low Temp. Phys.* **13**, 153 (1973).
- <sup>36</sup>R. Balzer and R. O. Simmons, in *Proceedings of the Thirteenth International Conference on Low-Temperature Physics*, 1972, edited by D. K. Timmerhaus, W. J. O'Sullivan, and E. F. Hammel, (Plenum, New York, 1974), Vol. 2, p. 115.
- <sup>37</sup>F. W. deWette, *Phys. Rev.* **129**, 1160 (1963).
- <sup>38</sup>R. C. Dynes and V. Narayanamurti, *Phys. Rev. B* **12**, 1731.
- <sup>39</sup>G. Ahlers (unpublished). These data were obtained in a different apparatus and with much higher temperature resolution than those reported in Refs. 14, 15.